

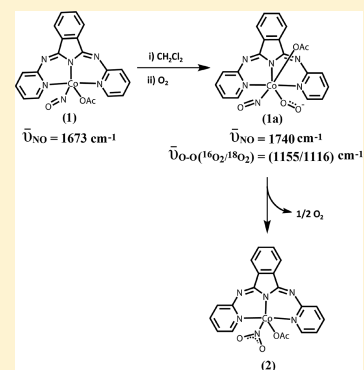
# Dioxygenation Reaction of a Cobalt-Nitrosyl: Putative Formation of a Cobalt–Peroxynitrite via a {Co<sup>III</sup>(NO)(O<sub>2</sub><sup>-</sup>)} Intermediate

Kuldeep Gogoi,<sup>†</sup> Soumen Saha,<sup>†</sup> Baishakhi Mondal,<sup>†</sup> Hemanta Deka,<sup>†</sup> Somnath Ghosh,<sup>†</sup> and Biplab Mondal<sup>\*,†</sup>

<sup>†</sup>Department of Chemistry, Indian Institute of Technology Guwahati, North Guwahati, Assam 781039, India

## Supporting Information

**ABSTRACT:** A cobalt-nitrosyl complex, [(BPI)Co(NO)(OAc)], **1** {BPI = 1,3-bis(2'-pyridylimino)isoindol} was prepared and characterized. Structural characterization revealed that the cobalt center has a distorted square pyramidal geometry with the NO group coordinated from the apical position in a bent fashion. The addition of dioxygen (O<sub>2</sub>) to the dichloromethane solution of complex **1** resulted in the formation of nitro complex, [(BPI)Co(NO<sub>2</sub>)(OAc)], **2**. It was characterized structurally. Kinetic studies suggested the involvement of an associative mechanism. FT-IR spectroscopic studies suggested the formation of the intermediate **1a** [(BPI)Co<sup>III</sup>(NO)(O<sub>2</sub><sup>-</sup>)(OAc)] in the reaction. The intermediate **1a** decomposed to complex **2** via a presumed peroxynitrite intermediate which was implicated by its characteristic phenol ring nitration reaction.



## INTRODUCTION

Nitric oxide (NO) is an important regulatory molecule in mammalian biology. It is known to play the key roles in diverse biological processes such as neurotransmission, immune response, and so on.<sup>1–4</sup> It has been found that the submicromolar concentrations of NO are sufficient for its functions, and an overproduction of it has a detrimental effect due to the formation of peroxynitrite anion (PN, ONOO<sup>-</sup>) and other secondary reactive nitrogen species which induce oxidative damage to DNA, lipids, proteins, and other structures.<sup>5,6</sup> Nitric oxide deoxygenases (NOD) are known to control the level of NO in biological systems. In NODs, the reaction of the Fe(III)-superoxide species with NO results in the biologically benign nitrate (NO<sub>3</sub><sup>-</sup>) ion.<sup>7</sup> This reaction is believed to proceed through the formation of a metal–peroxynitrite intermediate.<sup>7,8</sup> It is believed that peroxynitrite intermediate forms in the diffusion-controlled reaction between NO and superoxide anion or H<sub>2</sub>O<sub>2</sub> and nitrite (NO<sub>2</sub><sup>-</sup>) in the presence of the peroxidase enzymes.<sup>9</sup>

The biological relevance of NO inspires a wide range of studies of its coordination and interaction with transition metal centers and subsequently, their dioxygenation reaction. An extensive study has been done in this direction with the Fe-proteins and their models.<sup>7,10</sup> Recently, the examples involving other transition metal ions in the generation and reactivity of ONOO<sup>-</sup> are reported.<sup>11</sup> The Karlin's group reported the example of a peroxynitrite complex from the reaction of a mixed-valent nitrosyl complex of Cu(I)Cu(II), [Cu<sup>I</sup>II<sub>2</sub>(UN-O<sup>-</sup>)(NO)]<sup>2+</sup> with O<sub>2</sub>. It has been shown that the reaction resulted in the corresponding superoxide and nitrosyl adduct, [Cu<sup>II</sup><sub>2</sub>(UN-O<sup>-</sup>)(NO)(O<sub>2</sub><sup>-</sup>)]<sup>2+</sup>, in the first step, and it was subsequently converted to the corresponding peroxynitrite

complex.<sup>12</sup> A Cu-peroxynitrite intermediate was also proposed in the reaction of a Cu(I)-nitrosyl complex with O<sub>2</sub> to finally result in the corresponding NO<sub>2</sub><sup>-</sup>.<sup>13</sup> Recently, it has been shown that the reaction of Cu(II)-nitrosyl complexes with H<sub>2</sub>O<sub>2</sub> results in the copper-nitrate complexes via a presumed Cu-peroxynitrite intermediate.<sup>14</sup> The reaction of nonheme Cr(IV)-peroxo and Cr(III)-superoxo complexes with NO were reported to result in the presumed Cr(III)-peroxynitrite intermediate.<sup>15</sup> A Co-nitrosyl complex was reported to react with O<sub>2</sub> to result in the corresponding nitrite (NO<sub>2</sub><sup>-</sup>) product by Clarkson and Basolo.<sup>16</sup> The Co(III)-nitrosyl complexes of 12- and 13-membered *N*-tetramethylated cyclam ligands, [(12-TMC)Co<sup>III</sup>(NO)]<sup>2+</sup> and [(13-TMC)Co<sup>III</sup>(NO)]<sup>2+</sup> [12-TMC = 1,4,7,10-tetramethyl-1,4,7,10-tetraazacyclododecane] were reported to react with the superoxide ion resulting in the Co(II)-nitrite where the involvement of Co(III)-peroxynitrite intermediate was presumed.<sup>17</sup> Thus, the reaction of metal-nitrosyl complexes with O<sub>2</sub>, O<sub>2</sub><sup>-</sup>, or O<sub>2</sub><sup>2-</sup> is of potential interest from the NOD point of view. On the other hand, a pyrrole/imine ligand derived cobalt nitrosyl complex having {CoNO}<sup>8</sup> configuration has been shown to serve as potential HNO donor.<sup>18</sup>

The Co-nitrosyl complexes having {CoNO}<sup>8</sup> configuration has attracted attention because they can serve as the good replacement of {FeNO}<sup>8</sup> complexes which are inherently reactive.<sup>18</sup> On the other hand, cobalamins (Cbals) are known to react with NO to form nitrosocobalamins (NOCbals) in a diffusion-controlled rate and are believed to scavenge NO efficiently in vivo.<sup>19</sup> NOCbal is reported to react with O<sub>2</sub> to

Received: June 30, 2017

result in nitrocobalamin through the formation of peroxyinitrite Co(III) intermediate.<sup>116,19</sup> In addition, the Co-containing systems are found to be more promising with respect to the observation of peroxyinitrite complexes.<sup>11</sup> We have demonstrated recently that a nitrosyl complex of Co-porphyrinate reacts with H<sub>2</sub>O<sub>2</sub> to result in Co(III)-nitrite.<sup>20</sup> Unlike the nitrosyls of Fe(II)-porphyrinate, this complex was inert toward dioxygen. The chemical evidence suggests the involvement of a putative peroxyinitrite intermediate in the reaction. A Co(II) complex, [Co(L)<sub>2</sub>]Cl<sub>2</sub>, (L = bis(2-ethyl-4-methylimidazol-5-yl)methane) in methanol solution was shown to react with H<sub>2</sub>O<sub>2</sub> at -40 °C to result in the corresponding Co(III)-peroxo complex, [Co(L)<sub>2</sub>(O<sub>2</sub>)]<sup>+</sup>. The addition of NO gas to the this peroxo complex resulted in the Co(II)-nitrate complex.<sup>11g</sup> The putative formation of a Co(II)-peroxyinitrite intermediate was presumed based on the chemical evidence. No spectral evidence of formation of the peroxyinitrite intermediate was observed in these cases. In the present work, a cobalt(II) complex of a tridentate N-donor ligand, 1,3-bis(2'-pyridylimino)isoindol (BPI) (Figure 1) has been used for the

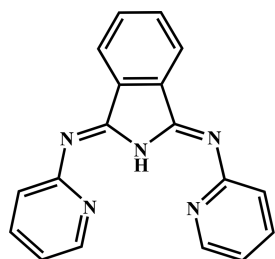


Figure 1. BPI ligand used for the present study.

preparation of nitrosyl complex followed by its study with dioxygen.<sup>21</sup> The spectral characterization and kinetics studies suggest that in the present study the reaction of the {CoNO}<sup>8</sup> complex with O<sub>2</sub> led to the formation of an unusual superoxide species, [(BPI)Co(NO)(O<sub>2</sub>-)]<sup>+</sup> which then resulted in the corresponding nitro product in subsequent step. Chemical evidence suggests the involvement of a putative peroxyinitrite intermediate in the process of decomposition of the [(BPI)-Co(NO)(O<sub>2</sub>-)]<sup>+</sup> to the nitro complex.

## RESULTS AND DISCUSSION

The ligand, 1,3-bis(2'-pyridylimino)isoindol (BPI) was prepared using the earlier reported procedure by Siegl and co-workers.<sup>21</sup> It was characterized using FT-IR, <sup>1</sup>H NMR spectroscopy, ESI-mass spectrometry and microanalysis (Experimental Section). These data matched well with the earlier reported one. The bubbling of NO gas to the degassed

methanol solution of the ligand followed by the addition of an equivalent amount of cobalt acetate, tetrahydrate resulted in the precipitation of the Co(II)-nitrosyl complex, [(BPI)Co(NO)(OAc)] (1) (Scheme 1 and Experimental Section). It was isolated as solid and characterized by spectroscopic analyses as well as by single crystal X-ray structure determination. The ORTEP diagram of complex 1 is shown in Figure 2. The

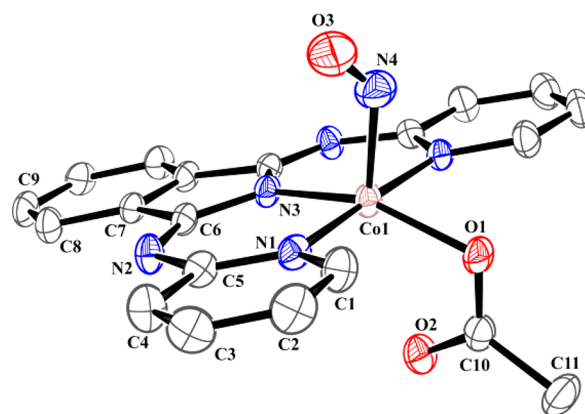
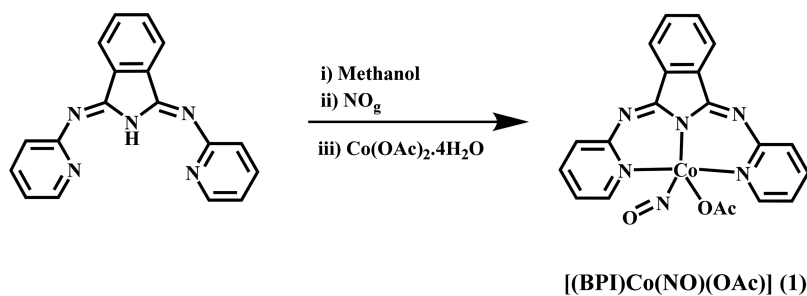


Figure 2. ORTEP diagram of complex 1 with 35% ellipsoid probability (H atoms and solvent molecule are not shown for clarity).

crystallographic data and metric parameters are listed in the Supporting Information (Tables S1–S3). The crystal structure revealed that the cobalt center is coordinated by the three N atoms from BPI, one acetate, and one NO group in a distorted square pyramidal geometry. The O atom from monodentate acetate group and the three N atoms from the BPI moiety formed the square plane and the NO group is coordinated from the apical position. The Co–N<sub>NO</sub> distance is 1.828(8) Å. The N–O distance and the Co–N–O angle were 1.014(8) Å and 132.7(7)°, respectively. Though the Co–NO distance is within the range of other reported values in analogous complexes, the N–O distance is relatively shorter.<sup>17,22</sup> It is to be noted that the structure has some inherent disorder in the N–O group, and it was refined with different N–O bond distances. However, no appreciable change in the crystal parameters was observed (Supporting Information, Table S4). Thus, it is difficult to assign the exact N–O bond distance in complex 1. Refinement with reassigning the electron density outside the coordination sphere too did not alter the crystal parameters to much extent. The bent geometry of the cobalt-nitrosyl, 1, is consistent with the {CoNO}<sup>8</sup> configuration as per the Enemark–Feltham notation.<sup>23</sup>

In the cases of recently structurally characterized Co-nitrosyl complexes of 12- and 13-membered N-tetramethylated cyclam

### Scheme 1. Synthesis of Complex 1



ligands,  $[(12\text{-TMC})\text{Co}(\text{NO})]^{2+}$  and  $[(13\text{-TMC})\text{Co}(\text{NO})]^{2+}$ , the Co–N–O angles are 128.5 and 124.4°; whereas, the N–O distances are 1.155 and 1.159 Å, respectively.<sup>17b</sup> In Co(II)-nitrosyl complex of  $N^1$ -(2,4,6-trimethylbenzyl)- $N^2$ -(2-(2,4,6-trimethylbenzyl)amino)ethyl-1,2-diamine ligand having {CoNO}<sup>8</sup> description, the Co–NO distance was reported to be 1.765(10) Å; whereas, the N–O distance and Co–N–O angles were 1.103(9) Å and 124.6(10)°.<sup>24</sup> In this 5-coordinated square pyramidal Co(II)-nitrosyl, the NO stretching frequency appeared at 1659 cm<sup>-1</sup>.<sup>24</sup> In FT-IR spectrum of complex **1**, the NO stretching frequency appeared at 1673 cm<sup>-1</sup>. However, in the case of  $[(12\text{-TMC})\text{Co}(\text{NO})]^{2+}$  and  $[(13\text{-TMC})\text{Co}(\text{NO})]^{2+}$ , the nitrosyl stretching frequency appeared at 1712 and 1716 cm<sup>-1</sup>, respectively, in acetonitrile solution.<sup>17b</sup> The complex **1** was silent in the X-band EPR spectroscopy which is consistent with its {CoNO}<sup>8</sup> description (Supporting Information, Figure S6). The ESI-Mass spectrum of the complex **1** was populated by the molecular ion peak at  $m/z$  387.28 which is assignable to the  $[(\text{BPI})\text{Co}(\text{NO})]^+$  unit (calculated  $m/z$ , 387.04) (Supporting Information, Figure S7). The observed isotopic distribution pattern was found to match well with the simulated one.

### ■ DIOXYGEN REACTIVITY OF COMPLEX **1**

In the UV–visible spectroscopy, dichloromethane solution of the complex **1** absorbs at 467 nm ( $\epsilon/M^{-1}\text{cm}^{-1}$ , 6230) and 348 nm ( $\epsilon/M^{-1}\text{cm}^{-1}$ , 12400) (Figure 3). The addition of O<sub>2</sub> gas to

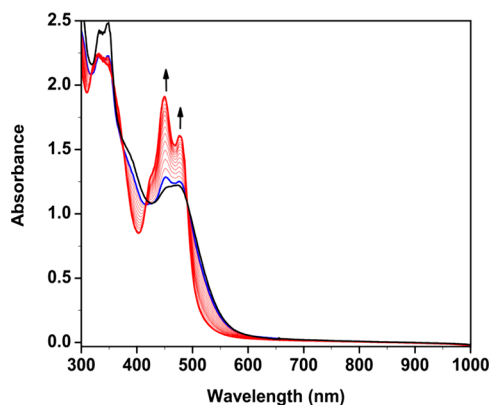


**Figure 3.** UV–visible spectra of complex **1** (black trace) and after addition of O<sub>2</sub> (blue trace; immediately after addition and red traces) in CH<sub>2</sub>Cl<sub>2</sub> at –20 °C.

the degassed dichloromethane solution of complex **1** at –20 °C resulted in the appearance of bands at 477 and 450 nm, respectively (Figure 3). The intensity of these bands were found to increase gradually with time and reached the maximum within 30 min of O<sub>2</sub> addition. The compound corresponding to this final spectrum was isolated as solid and characterized as complex **2** ( $(\text{BPI})\text{Co}(\text{NO}_2)(\text{OAc})$ ) (see Experimental Section). The kinetic studies revealed that the reaction of complex **1** with O<sub>2</sub> depends on the concentration of the added O<sub>2</sub> (Figure 4) suggesting the involvement of an associative mechanism.<sup>17a</sup> It is to be noted that the Co-nitrosyl complex of 14-membered N-tetramethylated cyclam ligands,  $[(14\text{-TMC})\text{Co}(\text{NO})]^{2+}$ , reacted with O<sub>2</sub> to result in  $[(14\text{-TMC})\text{Co}(\text{NO}_3)]^+$  in a dissociative pathway where the dissociation of NO group from the nitrosyl complex was proposed in the rate-determining step to form a cage intermediate,  $\{(14\text{-TMC})\text{Co}\cdots\text{NO}\}^{2+}$ , prior to the reaction

with O<sub>2</sub>.<sup>17a</sup> Thus, the overall rate of the reaction was independent of concentration of O<sub>2</sub>.

In the FT-IR spectrum, the addition of O<sub>2</sub> gas to the degassed dichloromethane solution of complex **1** resulted in the disappearance of the NO stretching frequency at 1673 cm<sup>-1</sup>, while a new band appeared at 1740 cm<sup>-1</sup> (Figure 5). This band was assigned to the NO stretching of the resulting intermediate, **1a** (Scheme 2). Recently, Karlin and co-workers reported that addition of O<sub>2</sub> gas to the dichloromethane solution of  $[\text{Cu}^{\text{II}}_2(\text{UN-O}^-)(\mu\text{-NO})]^{2+}$  resulted in the formation of  $[\text{Cu}^{\text{II}}_2(\text{UN-O}^-)(\text{NO})(\text{O}_2^-)]^{2+}$  where the NO stretching appeared at 1853 cm<sup>-1</sup>.<sup>12</sup> On the other hand, Theopold et al. reported that the reaction of a tris(3-*tert*-butyl-5-methylpyrazole)borate ligand derived cobalt(III) superoxo complex with NO at –78 °C resulted in the appearance of a new stretching band at 1849 cm<sup>-1</sup>, and it was assigned to the corresponding unstable nitrosyl intermediate.<sup>25</sup> It was reported earlier that in the case of cobalt(II)-nitrosyl complexes, the NO stretching frequency shifts ca. 100–150 cm<sup>-1</sup> upon oxidation of the cobalt(II) center to cobalt(III).<sup>26</sup> Thus, the addition of O<sub>2</sub> to the solution of complex **1** resulted in an intermediate where  $[\text{Co}^{\text{III}}\text{-NO}]$  is suggestive. In addition to the 1740 cm<sup>-1</sup> band, a new stretching frequency at 1155 cm<sup>-1</sup> was observed in the FT-IR spectrum (Figure 5). This frequency was sensitive to the <sup>18</sup>O<sub>2</sub> and found to shift to 1116 cm<sup>-1</sup> (Figure 6). It is to be noted that O<sub>2</sub> is known to bind with Co(II) and other transition metal ions in their reduced state to result in electron transfer reactions leading to the formation of corresponding Co(III)-superoxide complex.<sup>27</sup> The observed stretching frequency at 1155 cm<sup>-1</sup> is also suggestive to the formation of a metal-bound superoxide.<sup>27</sup> Hence the formulation of the intermediate complex **1a** as  $[(\text{BPI})\text{Co}^{\text{III}}(\text{NO})(\text{O}_2^-)]^+$  is logical (Scheme 2). Both the 1740 and 1155 cm<sup>-1</sup> bands disappeared with time and the appearance of two stretching frequencies at 1322 and 1297 cm<sup>-1</sup> assignable to the nitro group in complex **2** (Scheme 2) were observed.<sup>18,28</sup> The labeling experiment with <sup>18</sup>O<sub>2</sub> resulted in the shift of these characteristic frequencies to 1290 and 1271 cm<sup>-1</sup>, respectively, suggesting the incorporation of <sup>18</sup>O atom into the complex **2** (Figure S14; Supporting Information). It was further confirmed by isolation of complex **2** followed by structural characterization (see later). It is to be noted that the O<sub>2</sub> addition to the solution of complex **1** led to the formation of the superoxo species **1a** which is thermally unstable and decomposes to the corresponding nitro complex **2** quite fast. The spectrum, which we could manage to record with our existing facility, thus contains the stretching of the nitro product as impurity.

In UV–visible spectroscopic monitoring, the formation of the two new bands at 450 and 477 nm were observed which correspond to the decomposition product, complex **2**. The reaction proceeds through clean isosbestic points indicating the involvement of only one new species. No indication of formation of any intermediate was observed in the reaction even at –40 °C. This is perhaps because of the very fast reaction at the concentration of ca. 0.2 mM which was used for UV–visible study.

The complex **2** was isolated as solid and characterized by spectroscopic as well as by single crystal X-ray structure determination. The ORTEP diagram of complex **2** is shown in Figure 7.

The diamagnetic nature of the complex **2** is in agreement with the presence of trivalent Co center in it. In the ESI-mass spectrum of the complex **2**, the  $[(\text{BPI})\text{Co}(\text{NO}_2)]^+$  was

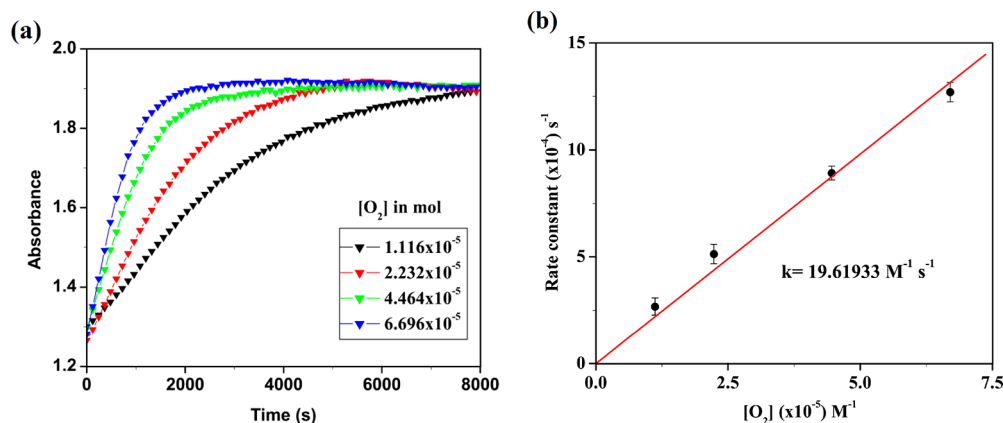


**Figure 4.** (a) Time versus absorbance plot at 450 nm for the reaction of complex **1** with different  $\text{O}_2$  concentrations in  $\text{CH}_2\text{Cl}_2$  at 298 K. (b)  $[\text{O}_2]$  concentration versus rate constant plot for the reaction of complex **1** with  $\text{O}_2$ .

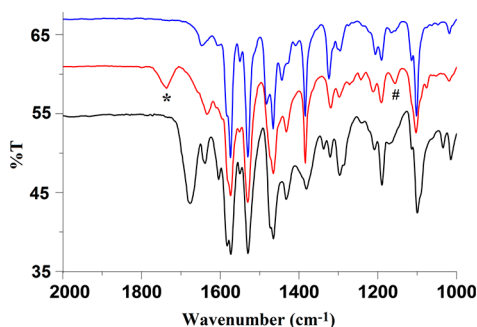
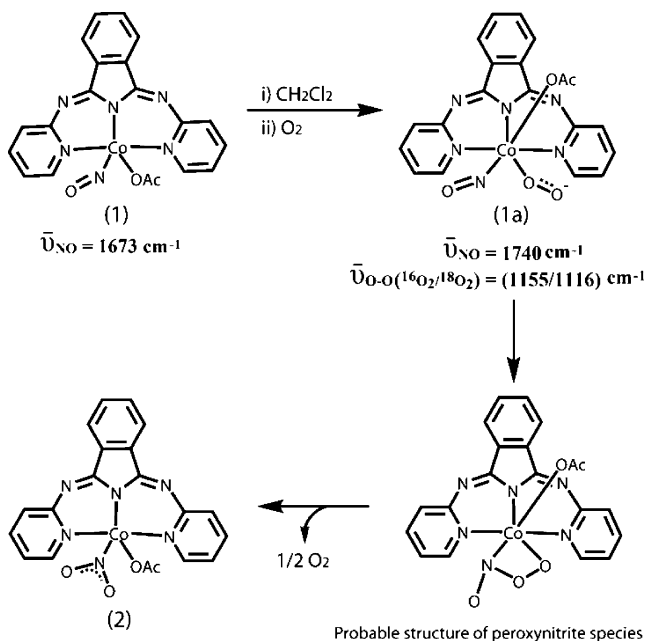


**Figure 5.** FT-IR spectra of complex **1** (black trace); immediately after addition of  $\text{O}_2$  (red trace;  $*v_{\text{NO}}$  shifted to  $1740\text{ cm}^{-1}$  and  $\#v_{\text{O-O}}$  appeared at  $1155\text{ cm}^{-1}$ ) and after 1/2 h of addition of  $\text{O}_2$  (blue trace) in  $\text{CH}_2\text{Cl}_2$  at  $-20\text{ }^\circ\text{C}$ .

### Scheme 2



observed at  $m/z$  403.06 (calculated 403.03). When the reaction was carried out with  $^{18}\text{O}_2$ , the molecular ion peak of complex **2** appeared at  $m/z$  405.10 (Figure S15; Supporting Information) suggesting the incorporation of one O atom from the added  $\text{O}_2$ .

The decomposition of the intermediate **1a** to the complex **2** presumably proceeds via the formation of a putative peroxynitrite intermediate, though no indication was observed in UV–visible studies. We sought chemical evidence to establish the formation of a peroxynitrite intermediate. In this regard, the nitration of the phenol ring has been reported extensively as evidence in favor of the formation of peroxynitrite intermediate.<sup>11b,e,f,16</sup> When the oxygenation reaction of complex **1** was carried out in the presence of 2,4-ditertiarybutyl phenol (DTBP), the formation of corresponding nitrophenol with a yield of ca. 42% (Experimental Section) was observed (Scheme 3). Though it is expected that the peroxynitrite intermediate will afford quantitative conversion of the phenol to nitrophenol, the parallel decomposition of the intermediate to complex **2** at the reaction temperature resulted in the formation of nitrophenol with a lower yield.

However, when DTBP was added in the reaction mixture after the addition of  $\text{O}_2$  in the solution of complex **1** at  $-20\text{ }^\circ\text{C}$ , the isolation of the products using chromatographic purification revealed the exclusive formation of complex **2** with unreacted DTBP (ca. 94%). Thus, it is implicated that the reaction of complex **1** with  $\text{O}_2$  resulted in the formation a peroxynitrite intermediate via complex **1a**. It should be noted that only complex **1** or **2** did not result in phenol ring nitration under experimental condition.

The decomposition of the presumed peroxynitrite intermediate to complex **2** could be envisaged either through the release of  $1/2\text{O}_2$  or via the mechanism proposed by Basalo where a peroxynitrite intermediate interacts with one unit of nitrosyl complex in fast step to result in  $-\text{N}-\text{O}-\text{O}-\text{N}-$  linkage which decomposed to two units of corresponding nitro complex.<sup>16</sup> Although, there is no direct evidence to confirm which mechanism is operating in the present case, considering the yield of isolated nitrophenol (ca. 42%), the first pathway seems more logical.

## EXPERIMENTAL SECTION

**Materials and Methods.** All reagents and solvents of reagent grade were purchased from commercial sources and used as received except specified. All the reactions were performed under inert conditions unless specified.  $^{18}\text{O}_2$  was purchased from Icon Isotopes. Deoxygenation of the solvent and solutions was effected by repeated vacuum/purge cycles or bubbling with argon for 30 min. UV–visible spectra were recorded on an Agilent Technologies Cary 8454 UV–visible spectrophotometer. FT-IR spectra of the samples were taken on a PerkinElmer spectrophotometer with samples prepared either as KBr

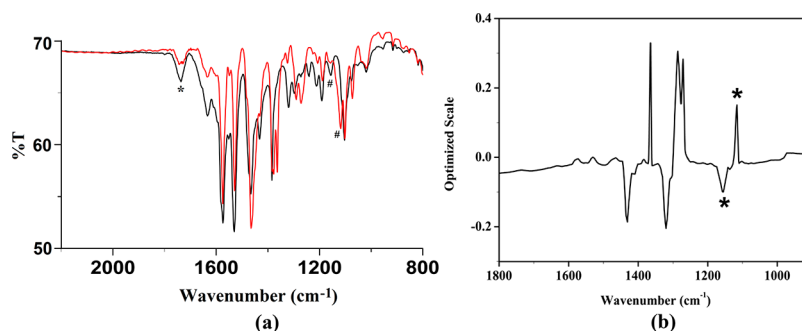


**Figure 6.** (a) FT-IR spectra of complex **1** immediately after addition of  $^{16}\text{O}_2$  (black trace;  $\nu_{\text{NO}}$  at  $1740\text{ cm}^{-1}$  and  $\nu_{\text{O-O}}$  at  $1155\text{ cm}^{-1}$ ) and upon labeling with  $^{18}\text{O}_2$  (red trace;  $\nu_{\text{O-O}}$  shifted to  $1116\text{ cm}^{-1}$ ) in  $\text{CH}_2\text{Cl}_2$  at  $-20\text{ }^\circ\text{C}$ . (b) Subtracted FT-IR spectrum of the reaction mixture obtained from the reaction of complex **1** with  $^{16}\text{O}_2$  and  $^{18}\text{O}_2$ , respectively, in  $\text{CH}_2\text{Cl}_2$  (\*stretching frequencies for coordinated O–O group). The other isotope-sensitive peaks are due to the presence of the decomposition product, complex **2**.

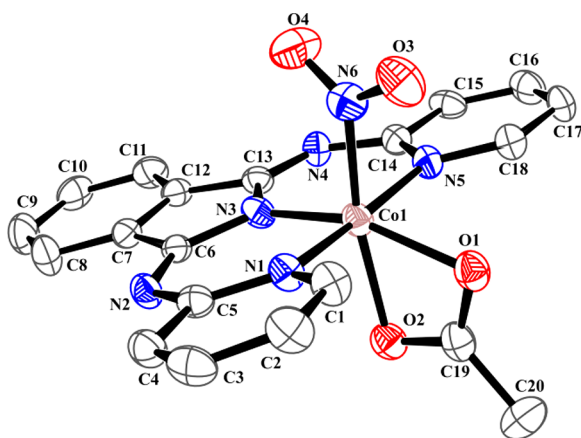
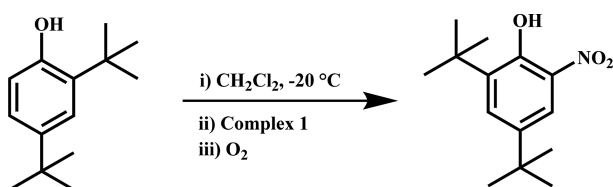


**Figure 7.** ORTEP diagram of complex **2** with 35% ellipsoid probability (H atoms are not shown for clarity).

### Scheme 3



pellets or in dichloromethane solution in KBr cell.  $^1\text{H}$  NMR spectra were recorded in 600 and 400 MHz Varian FT spectrometer. Chemical shifts (ppm) were referenced either with an internal standard ( $\text{Me}_4\text{Si}$ ) or to the residual solvent peaks. The X-band Electron Paramagnetic Resonance (EPR) spectra were recorded on a JES-FA200 ESR spectrometer, at room temperature with microwave power, 0.998 mW; microwave frequency, 9.14 GHz; and modulation amplitude, 2. Elemental analyses were obtained from a PerkinElmer Series II Analyzer.

**Kinetic Study.** The rates of the reactions of complex **1** with different  $\text{O}_2$  concentration were followed by monitoring the UV–visible spectral change of the solution using Agilent Technologies Cary 8454 UV–visible spectrophotometer installed with Chemstation kinetics software. The instrument was equipped with a Unisoku cryostat USP-203 B having thermostated cell holder. For the kinetic study, the temperature was regulated at  $25\text{ }^\circ\text{C}$ .  $\text{O}_2$  gas was diluted with Ar using EnviroNics Series 4040 computerized gas dilution system, and then the calculated amount was added to the reaction mixture through a gastight Hamilton syringe.

Single crystals were grown by slow evaporation of methanol and  $\text{CH}_2\text{Cl}_2$  solution of complexes **1** and **2**, respectively. The intensity data

were collected using a Bruker SMART APEX-II CCD diffractometer, equipped with a fine focus 1.75 kW sealed tube Mo  $K\alpha$  radiation ( $\lambda = 0.71073\text{ \AA}$ ) at  $273(3)\text{ K}$ , with increasing  $\omega$  (width of  $0.3^\circ$  per frame) at a scan speed of  $3\text{ s/frame}$ . The SMART software was used for data acquisition. Data integration and reduction were undertaken with SAINT and XPREP software.<sup>29</sup> Multiscan empirical absorption corrections were applied to the data using the program SADABS.<sup>30</sup> Structures were solved by direct methods using SHELXS-2014 and refined with full-matrix least-squares on  $F^2$  using SHELXL-2014/7.<sup>31</sup> Structural illustrations have been drawn with ORTEP-3 for Windows.<sup>32</sup>

**Synthesis of Ligand BPI [BPI = 1,3-bis(2'-pyridylimino)-isoindol].** Ligand BPI was synthesized following an earlier reported procedure with a minor modification.<sup>21</sup> A mixture of 1,2-dicyanobenzene (2.56 g; 20 mmol), 2-aminopyridine (3.95 g, 42 mmol) and  $\text{CaCl}_2$  (0.22 g, 2 mmol) in 30 mL of 1-butanol was refluxed for 48 h. Upon cooling to room temperature, the product began to precipitate. The precipitate was collected by filtration, washed with water, and recrystallized as pale yellow needles from ethanol/water. Yield: 4.42 g (ca. 74%). Elemental analyses for  $\text{C}_{18}\text{H}_{13}\text{N}_5$ : Calcd (%): C, 72.23; H, 4.38; N, 23.40. Found (%): C, 72.29; H, 4.36; N, 23.51. FT-IR (KBr pellet): 3061, 1631, 1582, 1457, 1429, 1305, 1259, 1220, 1034, 1098, 793  $\text{cm}^{-1}$ .  $^1\text{H}$  NMR: (600 MHz,  $\text{CDCl}_3$ ):  $\delta_{\text{ppm}}$ : 8.62–8.61 (1H, dd), 8.09–8.07 (1H, dd), 7.78–7.75 (1H, dt), 7.66–7.60 (1H, dd), 7.47–7.45 (1H, d), 7.13–7.11 (1H, ddd).  $^{13}\text{C}$  NMR: (150 MHz,  $\text{CDCl}_3$ ):  $\delta_{\text{ppm}}$ : 160.7, 154.0, 148.0, 138.3, 136.0, 131.9, 123.4, 122.8, 120.4. Mass ( $m/z$ ): calcd, 299.12; found, 300.03 ( $\text{M}+1$ ).

**Synthesis of Complex 1.** To an oversaturated solution of BPI (150 mg, 0.5 mmol) in 10 mL of methanol, NO gas was bubbled for 2 min followed by the addition of  $\text{Co}(\text{OAc})_2 \cdot 4\text{H}_2\text{O}$  (125 mg, 0.5 mmol) in methanol (ca. 10 mL). The reaction mixture was stirred for 5 min which resulted in a dark brown precipitate. The excess of NO gas was removed by bubbling with Ar. Then the precipitate was filtered using a Schlenk frit fitted in the Schlenk line. Finally precipitate was washed under Ar with degassed methanol to get the pure complex **1**. X-ray quality crystals complex **1** was obtained when the reaction mixture was allowed to stand for 1–2 days. Yield: 123 mg (55%). Elemental analyses for  $\text{C}_{20}\text{H}_{15}\text{CoN}_6\text{O}_3$ : Calcd (%): C, 53.82; H, 3.39; N, 18.83. Found (%): C, 53.73; H, 3.42; N, 18.90. UV–visible (dichloromethane):  $\lambda_{\text{max}}$  ( $\epsilon$ ,  $\text{M}^{-1}\text{ cm}^{-1}$ ): 467 nm (6230), 348 nm (12400). FT-IR (KBr pellet): 2962, 1673 ( $\nu_{\text{NO}}$ ), 1637, 1581, 1529, 1465, 1261, 1098, 1017, 801  $\text{cm}^{-1}$ .  $^1\text{H}$ -NMR (400 MHz,  $\text{CDCl}_3$ )  $\delta$  8.94 (d,  $J = 6.4$  Hz, 2H), 8.17–8.13 (m, 2H), 8.05 (t,  $J = 7.4$  Hz, 2H), 7.84 (d,  $J = 8.3$  Hz, 2H), 7.66–7.63 (m, 2H), 7.37 (t,  $J = 6.3$  Hz, 2H), 2.08 (s, 3H). Mass ( $m/z$ ): calcd for  $[\text{Co}(\text{BPI})(\text{NO})]^+$ , 387.04; found, 387.28.

**Synthesis of Complex 2.** To a degassed solution of complex **1** (89 mg, 0.2 mmol) in dichloromethane (ca. 20 mL), an excess of  $\text{O}_2$  gas was bubbled for 1 min. The solution was then allowed to stir for 2 h at room temperature. The resulting light red solution was dried under vacuum and light brown solid of complex **2** was obtained. It was crystallized by slow evaporation of a dichloromethane solution. Yield: 85 mg (92%). Elemental analyses for  $\text{C}_{20}\text{H}_{15}\text{CoN}_6\text{O}_4$ : Calcd (%): C,

51.96; H, 3.27; N, 18.18. Found (%): C, 51.91; H, 3.29; N, 18.27. UV-visible (dichloromethane):  $\lambda_{\text{max}}$  ( $\epsilon$ ,  $\text{M}^{-1} \text{cm}^{-1}$ ): 477 nm (8200), 450 nm (9830), 329 nm (11200). FT-IR (KBr pellet): 2934, 1646, 1582, 1531, 1464, 1378, 1320, 1296, 1099, 1017, 953, 775  $\text{cm}^{-1}$ .  $^1\text{H}$  NMR (400 MHz,  $\text{CDCl}_3$ )  $\delta$  8.98 (d,  $J = 5.3$  Hz, 2H), 8.00 (s, 2H), 7.88 (t,  $J = 7.1$  Hz, 2H), 7.63 (d,  $J = 7.8$  Hz, 2H), 7.53 (d,  $J = 2.9$  Hz, 2H), 7.23–7.16 (m, 2H), 1.65 (s, 3H; contaminated with signal for trace of moisture). Mass ( $m/z$ ): calcd for  $[\text{Co}(\text{BPI})(\text{NO}_2)]^+$ , 403.03; found, 403.06.

**Reaction of Complex 1 with  $\text{O}_2$  in the Presence of 2,4-Di-*tert*-butylphenol: Isolation of 2,4-Di-*tert*-butyl-6-nitrophenol.** To a degassed solution of complex 1 (89 mg, 0.2 mmol) in 20 mL of dichloromethane was added 2,4-ditertiarybutylphenol (206 mg, 1 mmol); stirred for 5 min and the solution was cooled at  $-20$  °C.  $\text{O}_2$  gas was then bubbled through the solution for 1 min and the resulting mixture was stirred for 3 h at  $-20$  °C. The reaction mixture was then warmed to room temperature and dried under reduce pressure. The solid mass was then subjected to column chromatography using silica gel column and hexane as eluent to obtain 2,4-di-*tert*-butyl-6-nitrophenol (yield: 21 mg; 42%). Elemental analyses for  $\text{C}_{14}\text{H}_{21}\text{NO}_3$ , Calcd (%): C, 66.91; H, 8.42; N, 5.57. Found (%): C, 66.86; H, 8.43; N, 5.66.  $^1\text{H}$  NMR (600 MHz,  $\text{CDCl}_3$ ):  $\delta_{\text{ppm}}$  7.39 (s, 1H), 7.12 (s, 1H), 5.22 (s, 1H), 1.45 (s, 9H), 1.32 (s, 9H).  $^{13}\text{C}$  NMR (150 MHz,  $\text{CDCl}_3$ ):  $\delta_{\text{ppm}}$  150.0, 143.2, 136.4, 125.5, 125.0, 122.5, 35.4, 34.7, 31.9, 29.9. Mass ( $m/z$ ): calcd, 251.15; found, 250.47 (M–1).

## CONCLUSION

A cobalt-nitrosyl complex,  $[(\text{BPI})\text{Co}(\text{NO})(\text{OAc})]$ , **1** having  $\{\text{CoNO}\}^8$  description was prepared. Structural characterization revealed that NO is bonded to the cobalt center in a bent fashion with a relatively shorter N–O distance. The addition of dioxygen to the dichloromethane solution of complex **1** resulted in the formation of corresponding nitro complex,  $[(\text{BPI})\text{Co}(\text{NO}_2)(\text{OAc})]$ , **2**. Spectroscopic studies suggested the involvement of the intermediate **1a**  $[(\text{BPI})\text{Co}^{\text{III}}(\text{NO})(\text{O}_2^-)(\text{OAc})]$ . The complex **1a** decomposed to complex **2** via a presumed peroxynitrite intermediate which was implicated by its characteristic phenol ring nitration reaction.

## ASSOCIATED CONTENT

### Supporting Information

The Supporting Information is available free of charge on the ACS Publications website at DOI: 10.1021/acs.inorgchem.7b01673.

Spectral analyses, crystallographic data, and metric parameters of the complexes (PDF)

### Accession Codes

CCDC 1558935–1558936 contain the supplementary crystallographic data for this paper. These data can be obtained free of charge via [www.ccdc.cam.ac.uk/data\\_request/cif](http://www.ccdc.cam.ac.uk/data_request/cif), or by emailing [data\\_request@ccdc.cam.ac.uk](mailto:data_request@ccdc.cam.ac.uk), or by contacting The Cambridge Crystallographic Data Centre, 12 Union Road, Cambridge CB2 1EZ, UK; fax: +44 1223 336033.

## AUTHOR INFORMATION

### Corresponding Author

\*E-mail: [biplab@iitg.ernet.in](mailto:biplab@iitg.ernet.in). Phone: +91-361-258-2317. Fax: +91-361-258-2339.

### ORCID

Biplab Mondal: 0000-0002-0594-6749

### Notes

The authors declare no competing financial interest.

## ACKNOWLEDGMENTS

The authors would like to thank Department of Science and Technology, India for financial support (EMR/2014/000291); DST-FIST for X-ray diffraction facility.

## REFERENCES

- (1) Goyal, R. K.; Hirano, I. The enteric nervous system. *N. Engl. J. Med.* **1996**, *334*, 1106–1115.
- (2) Stark, M. E.; Szurszewski, J. H. Role of nitric oxide in gastrointestinal and hepatic function and disease. *Gastroenterology* **1992**, *103*, 1928–1949.
- (3) Jaffrey, S. R.; Snyder, S. H. Nitric oxide: a neural messenger. *Annu. Rev. Cell Dev. Biol.* **1995**, *11*, 417–440.
- (4) Bogdan, C. Nitric oxide and the immune response. *Nat. Immunol.* **2001**, *2*, 907–916.
- (5) (a) Riveros-Moreno, V.; Beddell, C.; Moncada, S. Nitric oxide synthase: Structural studies using anti-peptide antibodies. *Eur. J. Biochem.* **1993**, *215*, 801–808. (b) Ignarro, L. J. Biosynthesis and metabolism of endothelium-derived nitric oxide. *Annu. Rev. Pharmacol. Toxicol.* **1990**, *30*, 535–560. (c) Radi, R. Nitric oxide, oxidants, and protein tyrosine nitration. *Proc. Natl. Acad. Sci. U. S. A.* **2004**, *101*, 4003–4008.
- (6) (a) Liaudet, L.; Soriano, F. G.; Szabo, C. Biology of nitric oxide signaling. *Crit. Care Med.* **2000**, *28*, N37–N52. (b) Pacher, P.; Beckman, J. S.; Liaudet, L. Nitric oxide and peroxynitrite in health and disease. *Physiol. Rev.* **2007**, *87*, 315–424. (c) Beckman, J. S.; Koppenol, W. H. Nitric oxide, superoxide, and peroxynitrite: the good, the bad, and ugly. *Am. J. Physiol.* **1996**, *271*, C1424–C1437.
- (7) (a) Pfeiffer, S.; Gorren, A. C. F.; Schmidt, K.; Werner, E. R.; Hansert, B.; Bohle, D. S.; Mayer, B. Metabolic fate of peroxynitrite in aqueous solution. Reaction with nitric oxide and pH-dependent decomposition to nitrite and oxygen in a 2:1 stoichiometry. *J. Biol. Chem.* **1997**, *272*, 3465–3470. (b) Coddington, J. W.; Hurst, J. K.; Lymar, S. V. Hydroxyl radical formation during peroxynitrous acid decomposition. *J. Am. Chem. Soc.* **1999**, *121*, 2438–2443. (c) Koppenol, W. H.; Bounds, P. L.; Nauser, T.; Kissner, R.; Rieggger, H. Peroxynitrous acid: controversy and consensus surrounding an enigmatic oxidant. *Dalton Trans.* **2012**, *41*, 13779–13787. (d) Lymar, S. V.; Khairutdinov, R. F.; Hurst, J. K. Hydroxyl radical formation by O–O bond homolysis in peroxynitrous acid. *Inorg. Chem.* **2003**, *42*, 5259–5266. (e) Goldstein, S.; Lind, J.; Merényi, G. Chemistry of peroxynitrites as compared to peroxynitrates. *Chem. Rev.* **2005**, *105*, 2457–2470. (f) Molina, C.; Kissner, R.; Koppenol, W. H. Decomposition kinetics of peroxynitrite: influence of pH and buffer. *Dalton Trans.* **2013**, *42*, 9898–9905.
- (8) (a) Schopfer, M. P.; Wang, J.; Karlin, K. D. Bioinspired heme, heme/nonheme diiron, heme/copper, and inorganic NOx chemistry:  $\bullet\text{NO}_{(\text{g})}$  oxidation, peroxynitrite–metal chemistry, and  $\bullet\text{NO}_{(\text{g})}$  reductive coupling. *Inorg. Chem.* **2010**, *49*, 6267–6282. (b) Ouellet, H.; Ouellet, Y.; Richard, C.; Labarre, M.; Wittenberg, B.; Wittenberg, J.; Guertin, M. Truncated hemoglobin HbN protects *Mycobacterium bovis* from nitric oxide. *Proc. Natl. Acad. Sci. U. S. A.* **2002**, *99*, 5902–5907. (c) Gardner, P. R.; Gardner, A. M.; Martin, L. A.; Salzman, A. L. Nitric oxide dioxygenase: an enzymic function for flavohemoglobin. *Proc. Natl. Acad. Sci. U. S. A.* **1998**, *95*, 10378–10383. (d) Ford, P. C.; Lorkovic, I. M. Mechanistic aspects of the reactions of nitric oxide with transition-metal complexes. *Chem. Rev.* **2002**, *102*, 993–1018. (e) Gardner, P. R.; Gardner, A. M.; Brashear, W. T.; Suzuki, T.; Hvitved, A. N.; Setchell, K. D. R.; Olson, J. S. Hemoglobins dioxygenate nitric oxide with high fidelity. *J. Inorg. Biochem.* **2006**, *100*, 542–550.
- (9) (a) Qiao, L.; Lu, Y.; Liu, B.; Girault, H. H. Copper-catalyzed tyrosine nitration. *J. Am. Chem. Soc.* **2011**, *133*, 19823–19831. (b) van der Vliet, A.; Eiserich, J. P.; Halliwell, B.; Cross, C. E. Formation of reactive nitrogen species during peroxidase-catalyzed oxidation of nitrite. A potential additional mechanism of nitric oxide-dependent toxicity. *J. Biol. Chem.* **1997**, *272*, 7617–7625.

(10) (a) Kurtikyan, T. S.; Ford, P. C. Hexacoordinate oxy-globin models Fe(Por)(NH<sub>3</sub>)(O<sub>2</sub>) react with NO to form only the nitrito analogs Fe(Por)(NH<sub>3</sub>)(η<sup>1</sup>-ONO<sub>2</sub>), even at ~ 100 K. *Chem. Commun.* **2010**, *46*, 8570–8572. (b) Yokoyama, A.; Han, J. E.; Karlin, K. D.; Nam, W. An isoelectronic NO dioxygenase reaction using a nonheme iron(III)-peroxo complex and nitrosonium ion. *Chem. Commun.* **2014**, *50*, 1742–1744. (c) Skodje, K. M.; Williard, P. G.; Kim, E. Conversion of {Fe(NO)<sub>2</sub>}<sup>10</sup> dinitrosyl iron to nitrito iron(III) species by molecular oxygen. *Dalton Trans.* **2012**, *41*, 7849–7851.

(11) (a) Roncaroli, F.; Videla, M.; Slep, L. D.; Olabe, J. A. New features in the redox coordination chemistry of metal nitrosyls{M–NO<sup>+</sup>; M–NO<sup>•</sup>; M–NO–(HNO)}. *Coord. Chem. Rev.* **2007**, *251*, 1903–1930. (b) Maiti, D.; Lee, D. – H.; Narducci Sarjeant, A. A.; Pau, M. Y. M.; Solomon, E. I.; Gaoutchenova, K.; Sundermeyer, J.; Karlin, K. D. Reaction of a copper–dioxygen complex with nitrogen monoxide (•NO) leads to a copper(II)–peroxynitrite species. *J. Am. Chem. Soc.* **2008**, *130*, 6700–6701. (c) Goodwin, J. A.; Coor, J. L.; Kavanagh, D. F.; Sabbagh, M.; Howard, J. W.; Adamec, J. R.; Parmley, D. J.; Tarsis, E. M.; Kurtikyan, T. S.; Hovhannisyian, A. A.; Desrochers, P. J.; Standard, J. M. Catalytic dioxygen activation by (nitro)(meso-tetrakis(2-N-methylpyridyl)porphyrinato)cobalt(III) cation derivatives electrostatically immobilized in nafion films: An experimental and DFT investigation. *Inorg. Chem.* **2008**, *47*, 7852–7862. (d) Kurtikyan, T. S.; Eksuzyan, S. R.; Goodwin, J. A.; Hovhannisyian, G. S. Nitric oxide interaction with oxy–coboglobin models containing trans-pyridine ligand: two reaction pathways. *Inorg. Chem.* **2013**, *52*, 12046–12056. (e) Herold, S.; Koppenol, W. H. Peroxynitritometal complexes. *Coord. Chem. Rev.* **2005**, *249*, 499–506. (f) Subedi, H.; Brasch, N. E. Mechanistic studies on the reaction of nitroxylcobalamin with dioxygen: evidence for formation of a peroxynitritocob(III)alamin intermediate. *Inorg. Chem.* **2013**, *52*, 11608–11617. (g) Saha, S.; Ghosh, S.; Gogoi, K.; Deka, H.; Mondal, B.; Mondal, B. Reaction of a cobalt(III)-peroxo complex and NO: Formation of a putative peroxynitrite intermediate. *Inorg. Chem.* **2017**, *56*, 10932–10938.

(12) Cao, R.; Elrod, L. T.; Lehane, R. L.; Kim, E.; Karlin, K. D. A peroxynitrite dicopper complex: Formation via Cu–NO and Cu–O<sub>2</sub> intermediates and reactivity via O–O cleavage chemistry. *J. Am. Chem. Soc.* **2016**, *138*, 16148–16158.

(13) Park, G. Y.; Deepalatha, S.; Puiiu, S. C.; Lee, D.-H.; Mondal, B.; Narducci Sarjeant, A. A.; del Rio, D.; Pau, M. Y. M.; Solomon, E. I.; Karlin, K. D. A peroxynitrite complex of copper: formation from a copper-nitrosyl complex, transformation to nitrite and exogenous phenol oxidative coupling or nitration. *JBIC, J. Biol. Inorg. Chem.* **2009**, *14*, 1301–1311.

(14) (a) Kalita, A.; Kumar, P.; Mondal, B. Reaction of a copper(II)–nitrosyl complex with hydrogen peroxide: putative formation of a copper(I)–peroxynitrite intermediate. *Chem. Commun.* **2012**, *48*, 4636–4638. (b) Kalita, A.; Deka, R. C.; Mondal, B. Reaction of a copper(II)–nitrosyl complex with hydrogen peroxide: phenol ring nitration through a putative peroxynitrite intermediate. *Inorg. Chem.* **2013**, *52*, 10897–10903.

(15) (a) Yokoyama, A.; Han, J. E.; Cho, J.; Kubo, M.; Ogura, T.; Siegler, M. A.; Karlin, K. D.; Nam, W. Chromium(IV)–peroxo complex formation and its nitric oxide dioxygenase reactivity. *J. Am. Chem. Soc.* **2012**, *134*, 15269–15272. (b) Yokoyama, A.; Cho, K. – B.; Karlin, K. D.; Nam, W. Reactions of a chromium(III)-superoxo complex and nitric oxide that lead to the formation of chromium(IV)-oxo and chromium(III)-nitrito complexes. *J. Am. Chem. Soc.* **2013**, *135*, 14900–14903.

(16) (a) Clarkson, S. G.; Basolo, F. Reactions of some cobalt nitrosyl complexes with oxygen. *J. Chem. Soc., Chem. Commun.* **1972**, *0*, 670–671. (b) Clarkson, S. G.; Basolo, F. Study of the reaction of some cobalt nitrosyl complexes with oxygen. *Inorg. Chem.* **1973**, *12*, 1528–1534.

(17) (a) Kumar, P.; Lee, Y.-M.; Hu, L.; Chen, J.; Park, J. Y.; Yao, J.; Chen, H.; Karlin, K. D.; Nam, W. Factors that control the reactivity of cobalt(III)–nitrosyl complexes in nitric oxide transfer and dioxygenation reactions: a combined experimental and theoretical investigation. *J. Am. Chem. Soc.* **2016**, *138*, 7753–7762. (b) Kumar, P.; Lee, Y.-M.;

Park, Y. J.; Siegler, M. A.; Karlin, K. D.; Nam, W. Reactions of Co(III)-nitrosyl complexes with superoxide and their mechanistic insight. *J. Am. Chem. Soc.* **2015**, *137*, 4284–4287.

(18) Rhine, M. A.; Rodrigues, A. V.; Urbauer, R. J. B.; Urbauer, J. L.; Stemmler, T. L.; Harrop, T. C. Proton induced reactivity of NO<sup>–</sup> to form a {CoNO}<sup>8</sup> complex. *J. Am. Chem. Soc.* **2014**, *136*, 12560–12563.

(19) Wolak, M.; Zahl, A.; Schnepfenseper, T.; Stochel, G.; van Eldik, R. Kinetics and mechanism of reversible binding of to the reduced cobalamin B<sub>12r</sub> (Cob(II)alamin). *J. Am. Chem. Soc.* **2001**, *123*, 9780–9791.

(20) Saha, S.; Gogoi, K.; Mondal, B.; Ghosh, S.; Deka, H.; Mondal, B. Reaction of a nitrosyl complex of cobalt porphyrin with hydrogen peroxide: putative formation of peroxynitrite intermediate. *Inorg. Chem.* **2017**, *56*, 7781–7787.

(21) (a) Siegl, W. O. Metal ion activation of nitriles. Syntheses of 1,3-bis(arylimino)isoindolines. *J. Org. Chem.* **1977**, *42*, 1872–1878. (b) Siegl, W. O.; Ferris, F. C.; Mucci, P. A. A convenient synthesis of 3- and 4-methylphthalonitrile. *J. Org. Chem.* **1977**, *42*, 3442–3443. (c) Siegl, W. O. Metal-chelating 1,3-bis(2'-pyridylimino)isoindolines. *J. Heterocycl. Chem.* **1981**, *18*, 1613–1618. (d) Hanson, K.; Roskop, L.; Djurovich, P. I.; Zahariev, F.; Gordon, M. S.; Thompson, M. E. A paradigm for blue- or red-shifted absorption of small molecules depending on the site of π-extension. *J. Am. Chem. Soc.* **2010**, *132*, 16247–16255.

(22) (a) Kozhukh, J.; Lippard, S. J. Influence of tetraazamacrocyclic ligands on the nitric oxide reactivity of their cobalt(II) complexes. *J. Am. Chem. Soc.* **2012**, *134*, 11120–11123. (b) Franz, K. J.; Doerrer, L. H.; Spingler, B.; Lippard, S. J. Pentacoordinate cobalt(III) thiolate and nitrosyl tropocoronand compounds. *Inorg. Chem.* **2001**, *40*, 3774–3780. (c) Scott, M. J.; Lippard, S. J. Coupling of carbon monoxide to isocyanides and enones induced by alkyl Zr(IV) and Hf(IV) tropocoronand complexes. *J. Am. Chem. Soc.* **1997**, *119*, 3411–3412. (d) Villacorta, G. M.; Lippard, S. J. Tropocoronands: a versatile macrocyclic ligand system for mononuclear and binuclear metal complexes. *Pure Appl. Chem.* **1986**, *58*, 1474–1484. (e) Jaynes, B. S.; Doerrer, L. H.; Liu, S.; Lippard, S. J. Synthesis, tuning of the stereochemistry, and physical properties of cobalt(II) tropocoronand complexes. *Inorg. Chem.* **1995**, *34*, 5735–5744.

(23) Enemark, J. H.; Feltham, R. D. Principles of structure, bonding, and reactivity for metal nitrosyl complexes. *Coord. Chem. Rev.* **1974**, *13*, 339–406.

(24) Deka, H.; Ghosh, S.; Saha, S.; Gogoi, K.; Mondal, B. Effect of ligand denticity on the nitric oxide reactivity of cobalt(II) complexes. *Dalton Trans.* **2016**, *45*, 10979–10988.

(25) Thyagarajan, S.; Incarvito, C. D.; Rheingold, A. L.; Theopold, K. H. In pursuit of a stable peroxynitrite complex-NO<sub>x</sub> (x = 1–3) derivatives of Tp(t-Bu,Me)Co. *Inorg. Chim. Acta* **2003**, *345*, 333–339.

(26) (a) Richter-Addo, G. B.; Hodge, S. J.; Yi, G. B.; Khan, M. A.; Ma, T.; Van Caemelbecke, E.; Guo, N.; Kadish, K. M. Synthesis, characterization, and spectroelectrochemistry of cobalt porphyrins containing axially bound nitric oxide. *Inorg. Chem.* **1996**, *35*, 6530–6538. (b) Kini, A. D.; Washington, J.; Kubiak, C. P.; Morimoto, B. H. Spectroelectrochemical characterization of substituted cobalt nitrosyl porphyrins. *Inorg. Chem.* **1996**, *35*, 6904–6906.

(27) (a) Wang, C.-C.; Chang, H.-C.; Lai, Y.-C.; Fang, H.; Li, C.-C.; Hsu, H.-K.; Li, Z.-Y.; Lin, T.-S.; Kuo, T.-S.; Neese, F.; Ye, S.; Chiang, Y.-W.; Tsai, M.-Li.; Liaw, W.-F.; Lee, W.-Z. A structurally characterized nonheme cobalt-hydroperoxo complex derived from its superoxo intermediate via hydrogen atom abstraction. *J. Am. Chem. Soc.* **2016**, *138*, 14186–14189. (b) Fielding, A. J.; Lipscomb, J. D.; Que, L., Jr. Characterization of an O<sub>2</sub> adduct of an active cobalt-substituted extradiol-cleaving catechol dioxygenase. *J. Am. Chem. Soc.* **2012**, *134*, 796–799. (c) Huber, A.; Muller, L.; Elias, H.; Klement, R.; Valko, M. Cobalt(II) complexes with substituted salen-type ligands and their dioxygen affinity in N-N-dimethylformamide at various temperature. *Eur. J. Inorg. Chem.* **2005**, *8*, 1459–1467. (d) Fritch, J. R.; Christoph, G. G.; Schaefer, W. P. Crystal structure of μ-peroxo-bis-[(ethylenediamine)(diethylenetriamine) cobalt(III)] perchlorate. *Inorg. Chem.* **1973**, *12*, 2170–2175. (e) Schaefer, W. P.; Marsh, R.

- E. The molecular structure of a peroxo-bridged dicobalt cation. *J. Am. Chem. Soc.* **1966**, *88*, 178–179. (f) Gall, R. S.; Rogers, J. F.; Schaefer, W. P.; Christoph, G. G. The structure of a monomeric oxygen carrying cobalt complex: dioxygen-*N,N'*-(1,1,2,2-tetramethyl)ethylenebis(3-tert-butylsalicylideneiminato)(1-benzylimidazole)cobalt(II). *J. Am. Chem. Soc.* **1976**, *98*, 5135–5144. (g) Floriani, C.; Calderazzo, F. Oxygen adducts of schiff's base complexes of cobalt prepared in solution. *J. Chem. Soc. A* **1969**, 946–953. (h) Collman, J. P.; Gagne, R. R.; Kouba, J.; Ljusberg-Wahren, H. Reversible oxygen adduct formation in cobalt(II) picket fence porphyrins. *J. Am. Chem. Soc.* **1974**, *96*, 6800–6802. (i) Nguyen, A. I.; Hadt, R. G.; Solomon, E. I.; Tilley, T. D. Efficient C-H bond activations via O<sub>2</sub> Cleavage by a dianionic cobalt(II) complex. *Chem. Sci.* **2014**, *5*, 2874–2878. (j) Corcos, A. R.; Villanueva, O.; Walroth, R. C.; Sharma, S. K.; Bacsa, J.; Lancaster, K. M.; MacBeth, C. E.; Berry, J. F. Oxygen activation by Co(II) and redox non-innocent ligand: Spectroscopic characterization of a radical-Co(II)-superoxide complex with divergent catalytic reactivity. *J. Am. Chem. Soc.* **2016**, *138*, 1796–1799.
- (28) (a) Goodwin, J.; Kurtikyan, T.; Standard, J.; Walsh, R.; Zheng, B.; Parmley, D.; Howard, J.; Green, S.; Mardyukov, A.; Przybyla, D. E. Variation of oxo transfer reactivity of (nitro) cobalt picket fence porphyrin with oxygen-donating ligands. *Inorg. Chem.* **2005**, *44*, 2215–2223. (b) Wyllie, G. R. A.; Scheidt, W. R. Solid-state structures of metalloporphyrin NO<sub>x</sub> Compounds. *Chem. Rev.* **2002**, *102*, 1067–1089.
- (29) SMART, SAINT, and XPREP; Siemens Analytical X-ray Instruments Inc.: Madison, Wisconsin, 1995.
- (30) Sheldrick, G. M. SADABS: software for Empirical Absorption Correction; University of Gottingen, Institut fur Anorganische Chemieder Universitat: Gottingen, Germany, 1999.
- (31) Sheldrick, G. M. SHELXS-2014; University of Gottingen: Germany, 2014.
- (32) Farrugia, L. J. ORTEP-3 for Windows - a version of ORTEP-III with a Graphical User Interface (GUI). *J. Appl. Crystallogr.* **1997**, *30*, 565.